Indian Journal of Chemical Technology
Vol. 31, November 2024, pp. 889-901
DOI: 10.56042/ijct.v31i6.11062

Determination of kinetic parameters and thermal decomposition of Epoxy-Moringa gum biocomposite using thermogravimetric analysis

R. Nalini Suja[1]*, B. Sridevi[2] & M. Chitra[3]

[1]Department of Chemistry, Panimalar Engineering College, Chennai 600 123,Tamil Nadu, India

[2]Department of Chemistry, Presidency College, Chennai-600 005, Tamil Nadu, India

[3]Department of Chemistry, Chellammal Women's College, Chennai-600 032, Tamil Nadu, India

*E-mail: rnalinirichard@gmail.com

Received 10 May 2024; accepted 4 October 2024

The use of natural filler based composites in various applications is growing due to easy availability and eco-friendly nature of the natural fillers. In the present study, an epoxy based bio composite has been prepared using *Moringa oleifera* gum as bio filler in order to investigate thermal properties. The composites have been prepared by incorporating *Moringa oleifera* gum at different volume fractions (4%, 8%, 12%, 16%, 20% v/v). Hand layup technique is used to fabricate the composite material. Fourier Transform Infrared Spectroscopy confirmed the formation of epoxy Moringa gum composite. Using thermogravimetric analysis data, activation energy and regression values (R^2) for the second stage of epoxy Moringa composite degradation have been determined by Coats-Redfern integration methods which involves 13 different kinetic models. The energy of activation is in the range of 72 to 99 kJ/mol and frequency factor was in the range of $2.5x10^5$ to $7.69x10^7$ for second order model which was identified as the best fitted model with R^2 value close to 1. The results are also compared with Broido and Horowitz-Metzger models. As the volume percentage of Moringa gum increases, the activation energy, frequency factor, enthalpy, entropy and Gibbs free energy also increases which proves the thermal stability of the Epoxy Moringa gum biocomposite is superior to the epoxy resin. Thus Moringa gum can be used as a potential bio filler to produce gum based composites having high thermal stability and can be promoted widely in various engineering applications.

Keywords: Broido and Horowitz-Metzger models, Coats-Redfern, Epoxy composites, *Moringa oleifera* gum, Thermal decomposition

Introduction

The recent advancements in bio based polymers are remarkable from a technological point of view, showcasing remarkable growth in the use for variety of applications ranging from automobile industry to packaging industry. Polymer composite materials are desired due to their low cost, low density, high corrosion resistance, high resistance to heat, high resistant to oxidation, availability, easy fabrication process[1,2]. The demand for synthesising composites using green technology is rising sharply due to their substantial potential as structural components in architecture, automobiles, aerospace structures, construction etc. Hence growing environmental consciousness and global environmental regulations are notably driving both academic and industrial sectors towards advancing green composites that prioritize eco-friendly, sustainability and biodegradability[3,4]. The need for incorporating the particulate fillers with the polymer matrix was studied[5-7] and it was shown that the fillers are incorporated in the polymer to strengthen the thermal, electrical, magnetic, mechanical properties, flame retardancy etc. The utilization of poly ester composite made from 40% *Cissus quadrangularis* fiber and 1% Moringa gum particle in industrial and home appliances were studied by Balaji et al.[8].

It was reported that the use of wastes from walnut, mussel, and hazelnut shells as bio filler material in epoxy matrix enhanced the thermal stability of the composites. When comparing the composite to pure epoxy resin, it was noticed that the addition of mussel shell enhanced the composite's thermal properties[9]. The kinetic characteristics of epoxy glass fiber reinforced plastic[10] indicated that the conversion rate α determines the activation energy of FRP. A direct relationship between log A and Ea was identified on studying the kinetics of rice husks with polypropylene and tetrafluoroethylene-ethylene copolymer[11]. According to Nguyen and Nguyen [12], the

maximum mechanical strength and flame retardant characteristics have been identified in banana fiber-reinforced composites composed of epoxy. Additionally TGA and derivative TGA data displayed high thermal strength for 20 wt% fiber composites. Improvement in the impact and compressive strength was achieved by the combination of kenaf fibre and kevlar composite [13]. Analyses focused on composite made from date palm tree trunk filler and epoxy had superior thermal stability as demonstrated by the greater residue value of 22.45% [14]. The study on the degradation kinetics of epoxy mixed with varying weight percentages (10%, 15%, and 20%) of polystyrene, the reaction was determined to be first order. Higher level of polystyrene content higher the thermal stability, evidenced by the activation energy rising from 74.49 to 96.80 kJ/mol[15].

The first decomposition temperature jumped from 302°C to 310°C and T_g to 90°C when 4 wt% carbon black was added to epoxy resin[16]. According to Chinnasamy et al.[17], the T_g was increased and the thermal characteristics of modified kevlar/glass fiber composites were enhanced without compromising thermal stability. Endothermic peaks were recorded at 472℃, 511.9℃ and 536℃, respectively. Research by Salasinska et al[18], adding powdered nut shell to epoxy composite materials increased their thermal stability up to 355℃. The epoxy resin loaded with 10 wt% siloxane exhibits high glass transition temperature and thermal stability among all samples prepared, attributed to enhanced chain entanglement and increased cross-link density facilitated by γ-amino propyl triethoxy silane.[19]

Kinetic analysis is essential for identifying the changes in thermal degradation behaviour and stability of polymers on adding fillers [20]. The kinetic parameters of thermal degradation of biodegradable polymers were calculated using Coats-Redfern, Ozawa and Horowitz-Metzger methods, yielding comparable results [21]. Expanding the use of polymers in a variety of industry sectors requires improving their thermal stability. To examine the potential of these composites for use in outdoor applications thermal characteristics were widely studied. In several polymer composite applications, kinetic analysis is crucial for predicting the changes that occur during thermal degradation processes. Kinetic parameter evaluation such as frequency factor (A) and activation energy (Ea) are typically done using model-free methods. The reaction model utilizes a mathematical equation to establish the quantitative correlation between the rate and the degree of conversion. This approach offers an intuitive fitting method to identify the reaction mechanism by determining an appropriate reaction model. The thermal degradation behaviour of epoxy with the addition of 0 to 25 wt% carboxyl-terminated butadiene acrylonitrile, exhibited increased thermal stability and higher activation energy up to 20% CTBN content, with degradation proceeding via a 2nd order reaction process, determined through the Coats-Redfern formula using a best-fit analysis[22]. Korkut [23] figured the activation energies of walnut shell ranges from 45.6 to78.4 kJ mol^{-1} and compared the values with other models. Although the values obtained by the Horowitz-Metzger technique were marginally higher, the Arrhenius and Coats-Redfern methods showed a strong agreement. Suresh et al. [24] used Broido equation to compute the Ea value of plywood during the thermal degradation study. Compared to simple plywood and water-proof plywood, the fire retardant plywood has higher Ea in the second degradation stage, indicating that it is substantially more thermally stable and would not catch fire even at high temperature.

Investigations into thermal degradation are of significant interest as they help determine the thermal stability and characteristics of a compound, contributing to solutions for environmental issues. Thermal analysis methods, including the determination of kinetic parameters from TG data, have found crucial applications in various fields. One of the simplest experiments for determining the kinetics of thermal degradation is TG under non-isothermal conditions. The Coats–Redfern fitting model, a single heating rate method, is widely used to determine kinetic parameters due to its accuracy and efficiency, despite its complexity involving g(x) algebraic expressions. Studies on the pyrolysis of date palm waste using this method have shown superior and detailed results, making it a preferred approach for describing thermogravimetric data and models [25,26].

Moringa gum derived from moringa plant is a natural polysaccharide consisting glucoronic acid, galactose and arabinose in the proportion of 2:7:10, rhamnose is present in traces and also has highly branched non reducing sugars which are safer to use. Moringa gum is a gelling and suspending agent, good film forming and binding agent[27,28]. The moringa gum clay-polymer composite's high biosorptive capacity, reusability, biodegradability, and diverse functional

groups make it an ideal and promising technology for cost-effective, long-term removal of toxic heavy metals from aqueous systems [29]. PET+ Moringa fruit composites containing 20 wt% *Moringa oleifera* fruit fiber content exhibited higher mechanical and thermal properties compared to other fabricated composites due to good bonding between the matrix, making them suitable for packaging applications [30]. Researchers have used various parts of moringa such as leaf, wood, pods as bio fillers. Interest in industrial uses of composites reinforced with bio fillers has increased significantly, as the usage of biopolymers as a base for such composites is rising dramatically. Epoxy resins, while advantageous for their facile crosslinking at room temperature and strong affinity for other materials, suffer from poor degradability due to extensive crosslinking, which can be mitigated by incorporating bio-based fillers to enhance biodegradability. Among the various natural fillers available moringa gum is notable because of its anti microbial property, availability and low cost. This study, the first to report on thermokinetic parameter analysis using the Coats-Redfern, Broido and Horowitz models, investigates the thermal properties of biobased epoxy composites with natural Moringa gum filler, addressing a gap in the literature and aiming to enhance their thermal stability and suitability for outdoor applications. From the investigations, more suitable kinetic parameters to better describe the degradation process can be identified. By examining the feasibility of introducing low cost moringa gum into epoxy resin in varying compositions (4% – 20%) and focusing on thermal characterization, this work presents an experimental approach that could make these composites suitable for designing thermal reactors, creating hybrid composites, and removing toxic substances due to their sorption capacity.

Experimental Section

Material and method

The matrix LY556 epoxy resin and HY951 hardener were supplied by Sakthi fibres, Chennai and the filler Moringa gum from Vimal agencies, Kancheepuram. Epoxy resin with hardener in the ratio 10:1 was used. The Moringa gum filler obtained from the bark of Murungai or Moringai or Muringa plant was allowed to dry naturally before being ground into granular powder using a ball mill for five hours, resulting in a fine particle size of five to ten microns. It was subsequently stored at room temperature. Hand layup technique and moderate compression were used to produce the composite samples. Gum was added to the epoxy resin and hardener mixture at varying volume percentages of 4, 8, 12, 16 and 20%.The filler and matrix were continuously mixed for an hour using a mechanical mixer to guarantee equal dispersion of the gum. The stiff plate served as a covering for a silicon rubber mould. Once a specific amount of resin filler mixture had been put into the mold it was smoothed out using a brush. The stiff plate was fitted over it. In order to compress the composite laminate, a weight of 500–600 N was subsequently placed over the mold. After the laminates had cured, they were cut according to ASTM (American Society for Testing and Materials) specifications random directions to ensure uniformity of the test specimens.

Thermal studies

Using Thermogravimetric Analyzer NETZSCH STA 2500, thermal characteristics of produced polymer composites were measured from 30℃ to 600℃ using a heating rate of 10 °C/min under N_2 environment. A NETZSCH DSC 214 type device was used to do the differential scanning calorimetry (DSC) measurements. The tests are carried out from 30℃ to 600°C. Through the use of endo and exo peaks from DSC the information about thermal transition that might occur in polymer samples was obtained.

Kinetic parameters analysis from TG

The following Eq. (1) indicates the rate of thermal decomposition

$$\frac{d\alpha}{dt} = k(T)f(\propto) \quad \text{... (1)}$$

Here k(T) is rate constant which is considered as temperature function and f(α) is differential form of the reaction model as a function of conversion.
The conversion rate α is specified as,

$$\propto = w_0 - w_t / w_0 - w_\infty$$

Here w_0, w_t and w_∞ denote the initial mass, mass at time 't' and final mass of the reaction, respectively.

Rate of conversion for a decomposition reaction can be rewritten as follows

$$\frac{d\alpha}{dt} = A\ e^{-\frac{Ea}{RT}} f(\propto) \quad \text{... (2)}$$

On introducing β the heating rate in a non-isothermal condition,

$$\frac{dT}{dt} = \beta = \frac{dt}{d\propto} \times \frac{d\alpha}{dt} \quad \text{... (3)}$$

On combination of Eq. (2) and Eq. (3), the rate of conversion can now be written as:

$$\frac{d\alpha}{dt} = \frac{A}{\beta}\, e^{\frac{-Ea}{RT}}\, f(\propto) \quad \text{... (4)}$$

On integrating Eq. (4) with respect to T, the reaction rate under non isothermal conditions is given as:

$$g(\propto) = \frac{A}{\beta}\int_0^T e^{\frac{-Ea}{RT}} dT \quad \text{... (5)}$$

Coats–Redfern Procedure[31]

A new equation can be obtained on solving Eq. (5), when 2RT/E ≥1,

$$ln\frac{g(\propto)}{T^2} = ln\frac{AR}{\beta Ea} - \frac{Ea}{RT} \quad \text{... (6)}$$

A straight line is produced when taking ln g (α)/T^2 values on Y axis and 1000/T values on X axis. The slope (-Ea/R) and intercept ($ln\frac{AR}{\beta Ea}$) are utilized to compute the activation energy (Ea) and frequency factor (A), respectively.

Coats–Redfern Models for solid-state decomposition reaction [32]

The following models as shown in Table 1 were used in this study to compare the activation energy of all the percentage compositions of Moringa gum composites synthesized.

Broido Equation [33]

The Broido equation for non-isothermal single heating rate method is given as

$$\ln\left[\ln\left(\frac{1}{y}\right)\right] = -\left(\frac{Ea}{RT}\right) + \ln\frac{RZTm^2}{Ea\beta} \quad \text{... (7)}$$

Table 1 — Reaction models used to compare the activation energy

Reaction Model	Code	g(α)
Diffusion Models		
One Dimensional Diffusion(ODD)	D1	α^2
Diffusion control Model (Jander)	D3	$[1-(1-\alpha)^{1/3}]^2$
Diffusion control Model (Crank)	D4	$1-(2/3)\alpha-(1-\alpha)^{2/3}$
Reaction order Models		
1st order Model	F1	-ln (1-α)
2nd order Model	F2	$(1-\alpha)^{-1}$ -1
Geometrical Contraction Model		
Contracting cylinder Model	R2	$1-(1-\alpha)^{1/2}$
Contracting sphere Model	R3	$1-(1-\alpha)^{1/3}$
Acceleratory Rate equation Model		
Mampel Power Law (n=1/3)	$MPL^{1/3}$	$3[1-(1-\alpha)^{1/3}]$
Mampel Power Law (n=1/2)	$MPL^{1/2}$	$2\,[1-(1-\alpha)^{1/2}]$
Mampel Power Law (n=2/3)	$MPL^{2/3}$	$3/2\,[1-(1-\alpha)^{2/3}]$
Nucleation Model		
Avrami-Erofeev Equation (n=2)	A2	$[-\ln(1-\alpha)]^{1/2}$
Avrami-Erofeev Equation (n=3)	A3	$[-\ln(1-\alpha)]^{1/3}$
Avrami-Erofeev Equation (n=4)	A4	$[-\ln(1-\alpha)]^{1/4}$

Here $y = w_t - w_f / w_0 - w_f$

w_0, w_t and w_f stand for the sample's initial weight, weight at time 't' and final weight respectively. T_m is the temperature at which maximum weight loss rate acquired. A straight line with slope = -Ea/R is obtained on plotting ln(ln(1/y)) vs 1/T . Based on the linear line's slope obtained the energy of activation and from the intercept frequency factor for the composites were calculated.

Horowitz-Metzger equation [34]

Horowitz- Metzger equation for a first-order kinetic reaction can be expressed as,

$$\ln(-\ln(1-\propto)) = \frac{Ea\theta}{RTs^2} \quad \text{... (8)}$$

θ=T-Ts, Ts corresponds to maximum loss occurring temperature

A straight line with slope = -Ea/RTs^2 will be obtained on plotting $\ln(-\ln(1-\propto))$ vs θ for Horowitz Metzger model.

Regression analyses for all the aforementioned models have been performed for all the Moringa gum composites using Origin Pro software. A reaction model that shows the value of the correlation coefficient (R^2) close to 1 is better than other models. To study the thermal behaviour of epoxy Moringa gum composites heat of activation at the main decomposition (i.e second stage) stage are determined from TGA. The entropy (ΔS), enthalpy (ΔH) and Gibbs free energy (ΔG) for all the Moringa composites have been found using the following relations (9) – (10).

$$\Delta S = R \ln(Ah/K_B T) \quad \text{... (9)}$$

$$\Delta H = Ea - RT \quad \text{... (10)}$$

$$\Delta G = \Delta H - T\Delta S \quad \text{... (11)}$$

Where, K_B is Boltzmann constant = 1.3806×10^{-16} erg/deg/mol, R = 8.314 J/K/mol and h is Planck's constant = 6.625×10^{-27} erg/s

Results and Discussion

Infrared spectra

Fig. 1 shows the Infra-Red (IR) spectra for the moringa *gum*, epoxy resin and epoxy moringa gum composite material. For Moringa gum an extensive and robust band in the range of 3300 cm^{-1} can be found due to the presence of OH group in polysaccharides. Furthermore, a group of well-resolved moderate bands located in the 2800-2900 cm^{-1} range can be attributed to symmetric and asymmetric stretching vibrations of

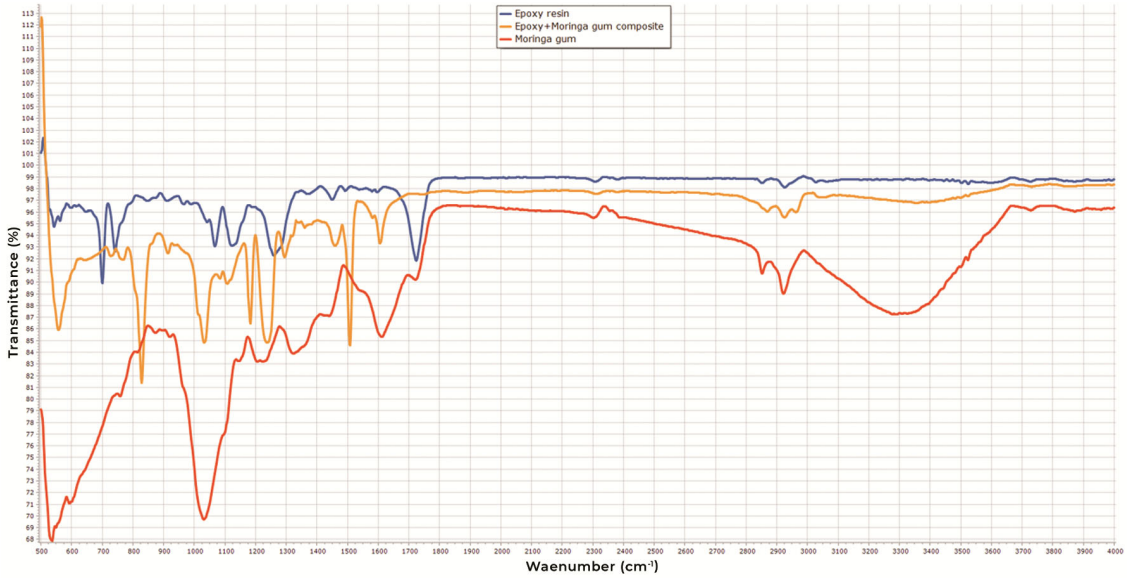

Fig. 1 — IR spectra of Moringa gum, Epoxy Resin, Epoxy Moringa gum Composite

skeletal CH and CH_2 in polysaccharides mainly arabinose (2920 cm^{-1})[35, 36]. The appearance of new band in the 1050 cm^{-1} is contributed to the formation of glycosidic bonds in polysaccharides. Thus from FTIR, the presence of carbohydrates in moringa gum is confirmed. For the epoxy resin LY556 the peaks at 2880 cm^{-1} are linked to the C-H stretching vibrations of the methyl group present where the two aromatic rings converge. Absorption at 2850 cm^{-1} is ascribed to the methylene group of the oxirane and 3030 cm^{-1} to the methene group of the oxirane. Absorption at 3098 cm^{-1} is linked to the methylene group present adjacent to the oxirane ring. The stretching vibrations of the aromatic moiety's C=C bonds are what cause the peak at 1480 cm^{-1}. The hydroxyl group is recognized as the origin of the broad peak at 3400 cm^{-1}. The broadness of the peak is due to intermolecular hydrogen bonding. The vibration absorption peaks at 909, 855-840 and 758 cm^{-1} are due to epoxy ring. At 1160 cm^{-1}, the ester's C-O stretching vibration is absorbed. The TETA hardener HY951 displays many peaks within the 3100-3350 cm^{-1} range, which can be traced to distinct stretching vibrations of the CH_2, NH_2, and NH bonds.

The formation of bio composite is revealed by the absence of peak of the oxirane moiety which vanished due to the ring opening reaction of the oxirane to form the bio composite. The peak at 1200 cm^{-1} corresponding to C-O-C stretching of aliphatic linear ester is attributed to the homo polymerization of epoxy group. Peak ascertained at 1225 cm^{-1} and 1020 $cm^{-1}$are analogous to the asymmetric aromatic C-O stretching and symmetric aromatic C-O stretching respectively, while the peak at 820 cm^{-1} indicates out of plane aromatic -CH deformation. Moreover, the appearance of peak at 1600 cm^{-1} specifies the asymmetric stretching vibration of carboxylate ion and C=O stretching is observed at 1680 cm^{-1} [27,28],.The sample also showed a good decrease in intensity of absorption which may be attributed to the presence of Moringa gum during composite preparation. During the formation of bio composite the epoxide ring opening processes is indicated by a strong and broad peak -OH stretching vibration at 3300 cm^{-1} is observed only for epoxy bio composite due to the presence of moringa gum in the composite material, which suggests that the polysaccharides and matrix surface had robust interfacial bonding.

Thermogravimetric Analysis

TGA is considered as the most practical and broadly available method to describe the thermal stability over a wide temperature range and also provides information about the behaviour of the composite under a constant gradual increase in temperature. Fig. 2 shows a typical thermogram and their derivative DTG for various compositions of Epoxy Moringa gum composite. The TGA curves were studied as weight loss percentage as a function of temperature ranges from 30°C to 600°C. The decomposition stages, range of decomposition,

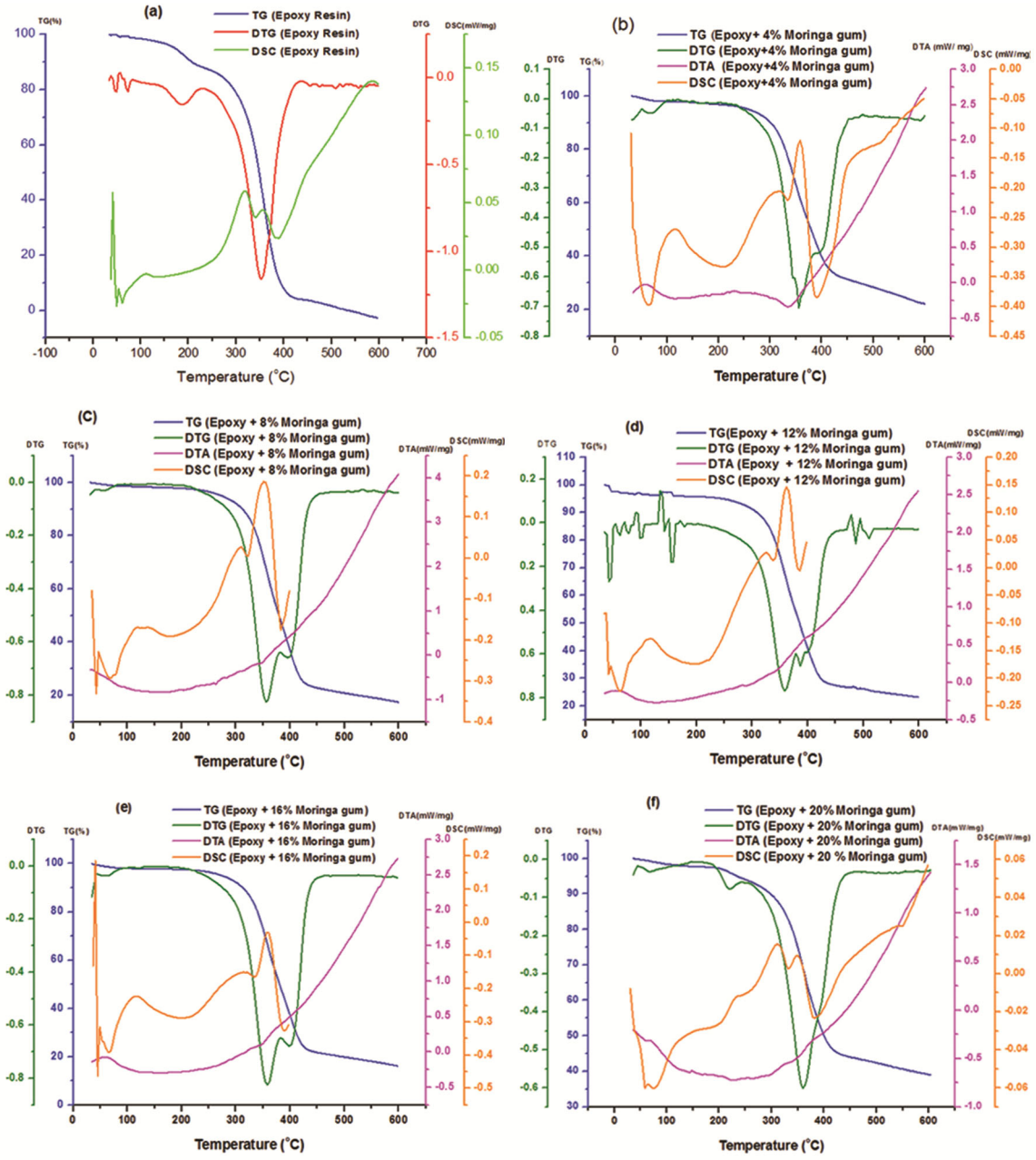

Fig. 2 — Graph of TG, DTG, DTA and DSC of (a) Epoxy Resin (b) Epoxy +4% Moringa gum composite (c) Epoxy +8% Moringa gum composite (d) Epoxy +12% Moringa gum composite (e) Epoxy +16% Moringa gum composite and (f) Epoxy +20% Moringa gum composite

maximum decomposition peak temperature of DTG are given in the Table 2.

From the TG graph, it was clear that all the epoxy *Moringa* gum composites underwent three stages of degradation and the mass losses at these stages were noted. The degradation mechanisms of all the composites were consistent, showing similar degradation profiles. The first stage of degradation, a drying stage occurred in 30-274°C temperature range with the mass loss of 4- 6.5 %. The weight of the composite is decreased due to the removal of bonded and free water content evaporated during the initial stages of heat treatment and volatile substances[37]. The second stage of weight loss occurs across a broad range of temperature 275-496°C with a major loss in weight of 65-75%. Degradation in this stage is maximum indicated the decomposition of significant parts of polysaccharides composed of D-mannose, D-xylose, D-galactose, D-glucuronic acid, L-arabinose, L-rhamnose. The presence of closely associated cross

Table 2 — Various Stages of decomposition of Epoxy Resin and composites

S. No	Sample	Stages	Decomposition Temperature Range(°C)	% Mass Loss	Residual Mass
1	Epoxy Resin	Stage 1	30-254	16.25	2.77
		Stage 2	255-460	75.05	
		Stage 3	461-600	5.93	
2	Epoxy+4% Moringa gum	Stage 1	30-259	5.87	8.4
		Stage 2	260-480	65.45	
		Stage 3	481-600	20.28	
3	Epoxy+8% Moringa gum	Stage 1	30-259	6.56	13.89
		Stage 2	260-485	68.91	
		Stage 3	486-600	10.64	
4	Epoxy+12% Moringa gum	Stage 1	30-264	5.93	14.52
		Stage 2	265-490	74	
		Stage 3	491-600	5.55	
5	Epoxy+16% Moringa gum	Stage 1	30-272	5.40	14.9
		Stage 2	273-492	75.12	
		Stage 3	493-600	4.58	
6	Epoxy +20% Moringa gum	Stage 1	35-274	4.22	20.5
		Stage 2	275-496	68.62	
		Stage 3	497-600	6.66	

linked polysaccharides in gum makes it rigid and difficult to decompose during thermal degradation. This matches with the result showed by Riya et al. on the thermal study of virgin moringa gum where maximum degradation occurred due to polysaccharides decomposition was at 301°C [38].

The TG curves confirmed the mass loss of 6 -23% in the third stage of dissolution at 497-600°C temperature ranges with the destruction of highly branched arabinogalactan, 1,6- and 1,3,6- linked galactopyranose units and 1,6- and 1,3,6- linked arabino furanose units, proteins present in it. Finally the residual mass contains the aromatic carbon in the epoxy matrix and the fillers. The residual mass formed for all the prepared epoxy moringa gum composites ranges from 5 to 20% which was far high when compared to 2.77% the residual mass of epoxy and also an indication for better thermal stability. In the thermal decomposition of the bio composite under study, their decomposition process gives mainly environmentally safer by products like small chain aliphatic hydrocarbon, alcohols, water, carbon-di-oxide and the products like benzene, toluene ,phenol, derivatives of phenols and amines and oxides of nitrogen from epoxy resin source. The findings were consistent with the literature [39,40].

From the graphs, It was noted that the thermal property of epoxy Moringa gum composite surpassed that of epoxy resin. As the concentration of Moringa gum increases in the bio composite, the particulate filler has reduced the bio composite weight loss at over 300°C and the bio composites' thermal stability boosted. Similar pattern was also observed in polyester composite with the increase in oil palm ash filler content by Ibrahim et al [41]. As the concentration of Moringa gum increases in the biocomposite, the onset of decomposition temperature also increases indicating improved thermal stability than the pure epoxy. T_{max} maximum decomposition temperature also increases proving enhanced thermal stability than the pure epoxy resin. The residual mass percentage also increases indicating increased thermal stability.

To estimate T_{max} precisely the first derivative TG (DTG) was taken. From the DTG curve, it was evident that as the percentage composition of Moringa gum filler increases the peak temperature also increases. On addition of Moringa gum filler to the neat epoxy resin the rigidity of the composite increases as the volume of the free spaces around the polymer chain decreases. As a result of this, the composite's density and thermal stability both increase. The addition of filler, particularly 20% Moringa gum, notably raises the peak temperature to 358.8°C in composites, comparison with the unreinforced epoxy resin's lower T max of 355.4°C. From 12% to 16 % the DTG peak temperature also changed from 358.3 °C to 358.4 °C, this small increase in peak temperature may be due to the effect of shear stress that is created when *Moringa* gum was mixed with epoxy resin by hand layup method.[15]

The DSC procedure was applied to determine the T_g of the all epoxy m*oringa* gum composites and epoxy resin and verified whether the addition of fillers caused any deviations. This study assessed the

T_g of neat epoxy resin and all the epoxy moringa gum composites containing 4%, 8%, 12%, 16%, and 20 vol% . Table 3 presents the T_g-onset, T_g-midpoint and T_g-end point temperatures for both the epoxy resin and the epoxy + Moringa gum composite formulations. As illustrated in Fig. 3, the average of the onset and end transition temperatures computed from the heat flow curves were employed to arrive at the T_g-midpoint temperatures.

It was observed that the virgin epoxy's T_g-midpoint was 59°C, which is in close accordance with the value listed in the manufacturer's information sheet (57.0°C). The addition of slightly lower percentage of Moringa gum to the epoxy matrix had a minimal impact on the polymer network, resulting in a minor rise in the T_g-midpoint compared to virgin epoxy. Thus it is evident from DSC curves that the glass transition temperature was higher than the epoxy resin, this is because the finely dispersed Moringa particles has penetrated the epoxy matrix and filled the gaps and hence reduced the free volume space. The T_g was further improved from 64.3°C to75.3°C when the Moringa gum content increased from 4% to 20%. The Moringa bonded with the epoxy resin increases the volume and hinders the rotation of molecules. This increased the density of the composite and made the composite more rigid ultimately increasing the thermal stability of the biocomposite. As the filler content is more, space occupied will be more which will weaken the mobility and further increase the T_g. It is well correlated with the results shown by Samuel at al [42] on incorporating areca fibre into epoxy matrix.

The DSC curve of epoxy resin without filler showed three endothermic peaks with no exothermic peak which is indicative of absence of cross linking in epoxy matrix. From the DSC, it is evident that for 8% Epoxy resin/*Moringa* gum there are 2 endothermic peaks followed by 2 exothermic peaks. The observed endothermic peak could be attributed to the removal of moisture from the epoxy composite. This moisture is likely absorbed on the composite's surface, where hydrogen bonding interactions occur between water molecules and the oxygen atoms of hydroxy and ether groups, as well as with the nitrogen atom of the amine group present in the epoxy composite moiety. The second endothermic peak may correspond to melting point temperature of the epoxy composite. There are 2 weak exothermic peaks which may be attributed to the cleavage of alkyl side chain and thermal degradation of polysaccharides present in Moringa gum.

The endothermic process below 100°C, corresponding to the evaporation of water molecules from liquid to a high kinetic energy gaseous state, was not prominently observed in DTA due to the subtlety of the peak. The DTA curves of Moringa bio composites showed endothermic peak with wide range of temperature with two non sharp peaks also called as shoulder peaks. The wide range observed corresponds to the decomposition processes of polysaccharides. It is plausible that the breakdown of polysaccharides occurs simultaneously, resulting in a broad endothermic peak. This trend is consistent across all compositions.

Kinetic Study Modelling

A quantitative analytical technique for figuring out a composite's thermal stability is the kinetic energy activation. Thermogravimetric analysis is a valuable tool for studying thermo-degradation kinetics, as it allows for the calculation of kinetic parameters such as activation energies and pre-exponential factors from a single thermogram using integral and

Table 3 — Weight loss calculation for epoxy and epoxy moringa gum composites

Material	10% loss in weight (°C)	20% loss in weight (°C)	30% loss in weight (°C)	40% loss in weight (°C)	50% loss in weight (°C)	60% loss in weight (°C)	DTG (°C)	T_g on set (°C)	T_g mid point (°C)	T_g end point (°C)
Pure Epoxy	207	295	323	338	350	356	355.4	44	59	74
Epoxy + 4% Moringa gum	300	330	349	360	378	394	355.7	40.5	64.3	88
Epoxy +8% Moringa gum	309	337	352	364	380	395	356	45.5	68.8	92
Epoxy +12 % Moringa gum	310	339	352	365	381	395	358.3	46	71	96
Epoxy +16% Moringa gum	312	339	355	369	384	399	358.4	52.5	75	97.5
Epoxy +20% Moringa gum	312	339	358	374	388	550	358.8	50.6	75.3	100

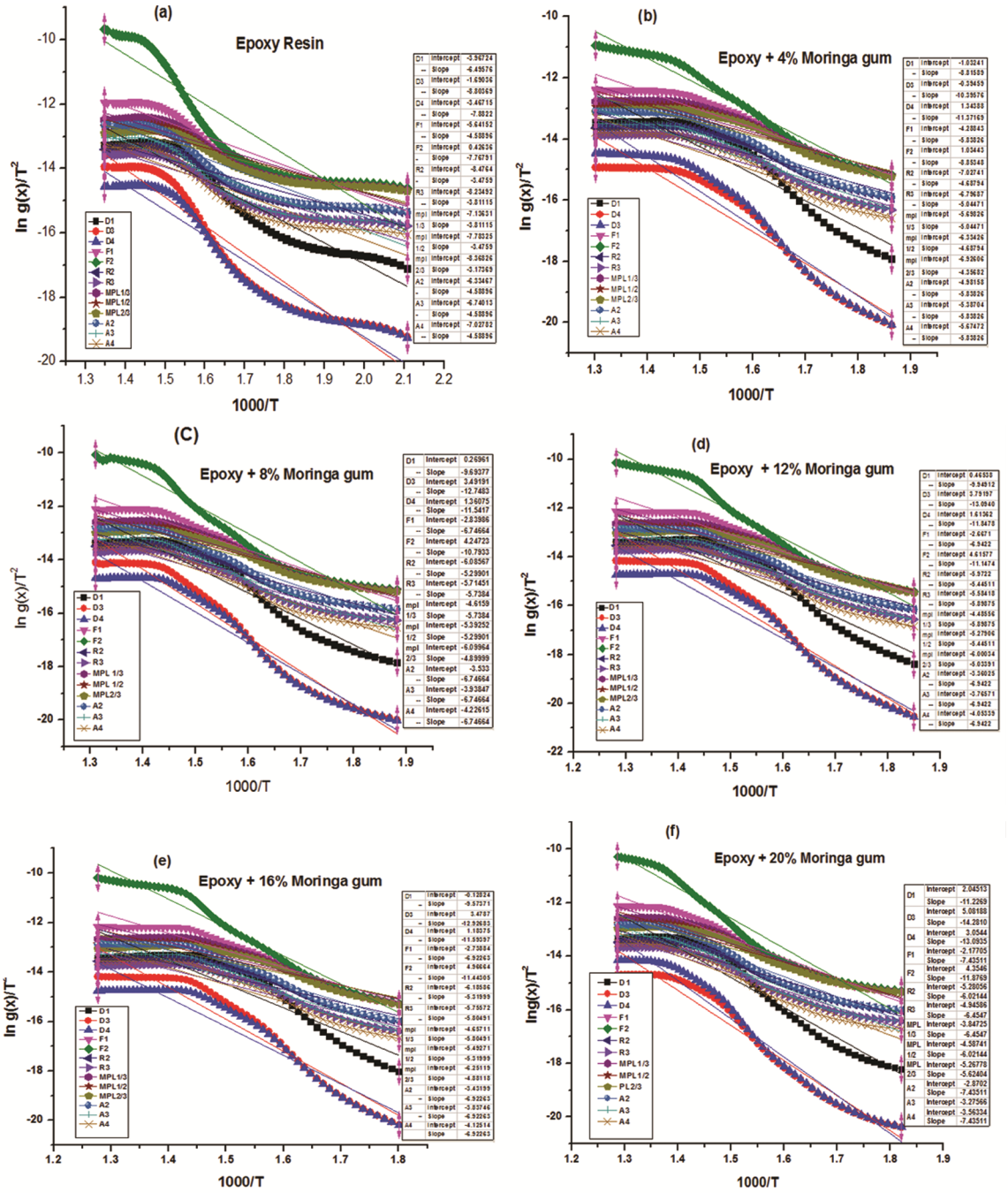

Fig. 3 — Plot of ln $g(x)/T^2$ Vs 1000/T for 13 models to calculate Ea (a) Neat Epoxy (b) Epoxy +4% Moringa gum composite (c) Epoxy+8% Moringa gum composite (d) Epoxy+12% Moringa gum composite (e) Epoxy+16% Moringa gum composite and (f) Epoxy+20% Moringa gum composite

differential methods. This information provides insights into decomposition kinetics and lifetime projections, which are crucial for preventing costly premature failures in actual end use. Material exhibiting high Ea can withstand high temperature without degradation and are thermally more stable. The kinetics of thermal degradation during the second stage of decomposition were studied, considering it as the major stage of the decomposition process following the increase in Initial Temperature of Decomposition (ITD) from 255°C to 275°C due to the addition of 20% filler in epoxy resin. [23,24].

Mathematical calculations were performed by Coats–Redfern, Broido and Horowitz–Metzger methods. The choices of these three specific methods ensure a comprehensive understanding of the thermal properties and stability of the composite. The formulae used in all the models are given in Table 4. On plotting ln $g(\alpha)/T^2$ versus 1000/T gave a straight line and is shown in Figs 3-5. From the slope and intercept values, the activation energy (Ea) and frequency factor (A) were calculated and the results are tabulated in Table 4. The composite's thermal stability is demonstrated by higher Ea. Material exhibiting high Ea can withstand high temperature without degradation and are thermally more stable [22].

Table 4 — Activation energy (Ea) and frequency factor (A) for epoxy composites

Code	Epoxy Resin	Epoxy + 4% Moringa gum	Epoxy + 8% Moringa gum	Epoxy + 12% Moringa gum	Epoxy + 16% Moringa gum	Epoxy + 20% Moringa gum
D1	Ea=54 $A=1.2x10^3$ $R^2=0.9310$	Ea= 73.29 $A=3.1x10^4$ $R^2=0.8843$	Ea=80.59 $A=1.3x10^5$ $R^2=0.9299$	Ea= 82.72 $A=1.6x10^5$ $R^2=0.8874$	Ea= 80.01 $A=8.4x10^4$ $R^2=0.8589$	Ea= 93.34 $A=8.7x10^5$ $R^2=0.9463$
D3	Ea=73.19 $A=1.6x10^4$ $R^2=0.9250$	Ea= 94.54 $A=4.4x10^4$ $R^2=0.9321$	Ea= 105.99 $A=4.2x10^6$ $R^2=0.9593$	Ea=108.86 $A=5.8x10^6$ $R^2=0.9378$	Ea=107.47 $A=4.2x10^5$ $R^2=0.9211$	Ea=118.73 $A=2.3x10^7$ $R^2=0.9693$
D4	Ea=65.53 $A=2.5x10^3$ $R^2=0.9289$	Ea= 86.43 $A=7.0x10^4$ $R^2=0.9166$	Ea= 95.95 $A=4.5x10^5$ $R^2=0.9504$	Ea=98.5 $A=5.9x10^5$ $R^2=0.921$	Ea=96.39 $A=3.8x10^5$ $R^2=0.9003$	Ea=108.86 $A=2.8x10^6$ $R^2=0.9625$
F1	Ea=38.15 $A=1.6x10^1$ $R^2=0.8975$	Ea= 48.54 $A=8.0x10^2$ $R^2=0.9378$	Ea=56.09 $A=3.9x10^4$ $R^2=0.9605$	Ea=57.72 $A=4.8x10^3$ $R^2=0.9472$	Ea=57.55 $A=4.5x10^3$ $R^2=0.9329$	Ea=61.82 $A=8.4x10^3$ $R^2=0.9699$
F2	Ea=64.58 $A=1.2x10^5$ $R^2=0.8829$	Ea=73.61 $A=2.5x10^5$ $R^2=0.9755$	Ea= 89.73 $A=7.6x10^6$ $R^2=0.9542$	Ea=92.68 $A=1.1x10^7$ $R^2=0.9733$	Ea=95.14 $A=1.7x10^7$ $R^2=0.9724$	Ea=98.74 $A=7.7x10^7$ $R^2=0.9874$
R2	Ea=28.89 $A=0.72x10^1 R^2=0.9067$	Ea=38.98 $A=4.2x10^2$ $R^2=0.8976$	Ea=44.06 $A=1.2x10^3$ $R^2=0.9411$	Ea=45.27 $A=1.4x10^2$ $R^2=0.9069$	Ea=44.23 $A=1.1x10^2$ $R^2=0.8823$	Ea=50.31 $A=3.1x10^2$ $R^2=0.9559$
R3	Ea=31.69 $A=1.01x10^1$ $R^2=0.9051$	Ea=41.94 $A=5.6x10^2$ $R^2=0.9126$	Ea=47.71 $A=1.9x10^3$ $R^2=0.9494$	Ea=49.04 $A=2.2x10^2$ $R^2=0.9224$	Ea=48.26 $A=1.8x10^2$ $R^2=0.9014$	Ea=53.66 $A=3.5x10^2$ $R^2=0.9621$
$MPL^{1/3}$	Ea=31.69 $A=3.03x10^1$ $R^2=0.9051$	Ea=41.94 $A=1.7x10^2$ $R^2=0.9126$	Ea=47.71 $A=5.7x10^2$ $R^2=0.9494$	Ea=49.04 $A=6.6x10^2$ $R^2=0.9224$	Ea=48.26 $A=5.5x10^2$ $R^2=0.9014$	Ea=53.66 $A=1.1x10^3$ $R^2=0.9621$
$MPL^{1/2}$	Ea=28.89 $A=1.45x10^1$ $R^2=0.90665$	Ea=38.98 $A=8.3x10^1$ $R^2=0.8976$	Ea=44.05 $A=2.4x10^2$ $R^2=0.9411$	Ea=45.27 $A=2.8x10^2$ $R^2=0.9069$	Ea=44.23 $A=2.2x10^3$ $R^2=0.8823$	Ea=50.06 $A=6.1x10^2$ $R^2=0.9559$
$MPL^{2/3}$	Ea=26.39 $A=0.74x10^1$ $R^2=0.9066$	Ea=36.22 $A=4.3x10^1$ $R^2=0.8809$	Ea=40.74 $A=1.1x10^2$ $R^2=0.931$	Ea=41.85 $A-1.2x10^2$ $R^2=0.8899$	Ea=40.58 $A=9.4x10^1$ $R^2=0.8612$	Ea=46.76 $A=2.9x10^2$ $R^2=0.9483$
A2	Ea=38.15 $A=8.1x10^1$ $R^2=0.8975$	Ea=48.54 $A=4.0x10^2$ $R^2=0.9378$	Ea=56.09 $A=7.9x10^2$ $R^2=0.9604$	Ea=57.78 $A=2.4x10^3$ $R^2=0.9472$	Ea=57.55 $A=2.2x10^3$ $R^2=0.9329$	Ea=61.82 $A=4.2x10^3$ $R^2=0.9699$
A3	Ea=38.15 $A=5.4x10^1$ $R^2=0.8975$	Ea=48.54 $A=2.7x10^2$ $R^2=0.9378$	Ea=56.09 $A=1.3x10^3$ $R^2=0.9604$	Ea=57.78 $A=1.6x10^3$ $R^2=0.9472$	Ea=57.55 $A=1.5x10^3$ $R^2=0.9329$	Ea=61.82 $A=2.81x10^3$ $R^2=0.9699$
A4	Ea=38.15 $A=4.07x10^1$ $R^2=0.8975$	Ea=48.54 $A=2.0x10^2$ $R^2=0.9378$	Ea=56.09 $A=9.9x10^2$ $R^2=0.964$	Ea=57.78 $A=1.2x10^3$ $R^2=0.9472$	Ea=57.55 $A=1.1x10^3$ $R^2=0.9329$	Ea=61.82 $A=2.11x10^3$ $R^2=0.9699$
Broido Model	Ea=57.98 $A=1.2x10^4$ $R^2=0.9517$	Ea=59.28 $A=9.11x10^3$ $R^2=0.9671$	Ea=67.38 $A=4.1x10^4$ $R^2=0.9724$	Ea=68.68 $A=4.5x10^4$ $R^2=0.9644$	Ea=68.74 $A=4.8x10^4$ $R^2=0.9548$	Ea=72.52 $A=5.07x10^4$ $R^2=0.9606$
Horowitz-Metzger model	Ea=67.56 $A=1.06x10^5$ $R^2=0.9566$	Ea=68.9 $A=2.7x10^4$ $R^2=0.9763$	Ea=70.46 $A=2.8x10^4$ $R^2=0.9862$	Ea=72.59 $A=2.9x10^4$ $R^2=0.9858$	Ea=73.85 $A=2.9x10^4$ $R^2=0.9858$	Ea=75.03 $A=2.9x10^4$ $R^2=0.9779$

Table 4 displayed an increase in activation energy of the composite compared to the resin, highlighting a greater energy demand to disrupt the bonding between the filler and the matrix, thus initiating the degradation process.

The model with high correlation coefficient R^2 corresponds to second order among all other models which gives reasonable energy of activation. Therefore, it can be considered that the second order reaction mechanism accurately depicts the second stage of decomposition in all of the composites that were prepared. The activation energy calculated from the Broido and Horowitz methods were in substantial agreement with the second order activation energy values. The table proved that as the weight percentage of Moringa gum increases the activation energy also increases because Moringa gum increases the stiffness and rigidity of the polymer chains which improves composite's thermal stability at high temperature. Calculated activation energy and frequency factor for the composites showed an analogues trend with respect to all the models. Frequency factor is associated to the number of collisions occurring between molecules with requisite orientation takes place successfully. Similar study conducted by Raza et al[26] showed increase in Ea from 101 kJ/mol to 171 kJ/mol using Coats Redfern method to predict the most resistive nature of date palm fibre polyvinyl alcohol composite. It was also identified by Zhang et al [43] that the introduction of wood floor content from 5 to 20% into HDPE composite increased Ea due to the prevention of heat flow by carbon formed during pyrolysis.

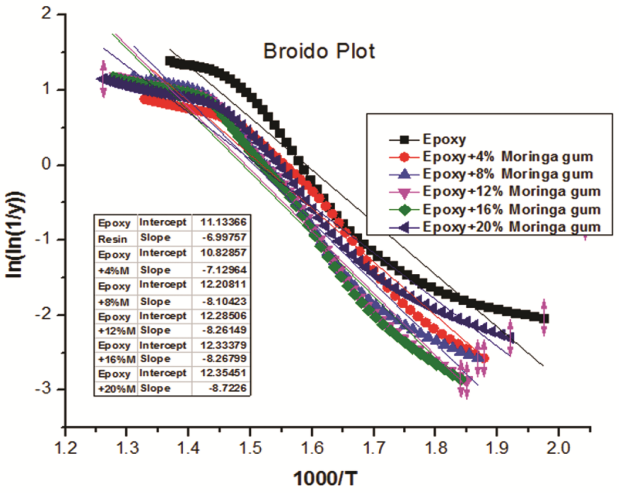

Fig. 4 — Broido plot to calculate Ea

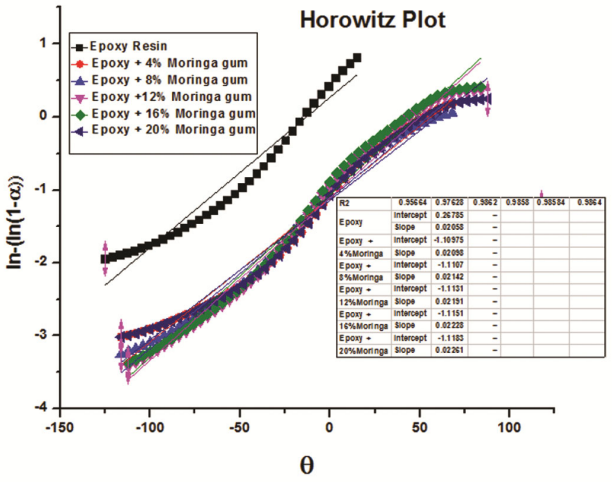

Fig. 5 — Horowitz Plot to calculate Ea

From the activation energy (Ea) and the frequency factor (A), change in enthapy (ΔH), change in entropy (ΔS) and change in free energy (ΔG) were calculated using Eqs 8-10.The results of kinetic data and the thermodynamic parameters for epoxy Moringa gum biocomposites are shown in Table 5. The weight percentage of Moringa gum influences the reaction rate constant, entropy, enthalpy and free energy. The enthalpy of 68-93 kJ/mol and the Gibbs free energy of 156-161 kJ/mol were obtained via the best-fitting model (F2). The positive enthalpy change indicated that the reaction is endothermic, requiring energy as shown by the heat flow graph, and that the composites are more stable compared to the resin. Each of the prepared composite showed a positive ΔG value, confirming that the reaction is not spontaneous, leading to an increase in the system's total energy. The magnitude of ΔG shows how far the reaction is from equilibrium, with larger values indicating a

Table 5 — Thermodynamic properties for thermal decomposition of epoxy composites

Composite percentage	Activation energy Ea (kJ/mol)	Frequency factor, A (s^{-1})	ΔH (kJ/mol)	ΔS (J/mol)	ΔG (kJ/mol)
Epoxy Resin	64.58	$1.19x10^5$	59.35	-153.9	156.1
Epoxy+4% Moringa gum	73.61	$2.49x10^5$	68.38	-147.8	161.3
Epoxy + 8% Moringa gum	89.73	$7.55x10^6$	84.50	-119.4	159.6
Epoxy + 12% Moringa gum	92.68	$1.13x10^7$	87.43	-116.1	160.7
Epoxy + 16% Moringa gum	95.14	$1.64x10^7$	89.89	-113	161.2
Epoxy + 20% Moringa gum	98.74	$7.69x10^7$	93.49	-100.2	156.8

greater shift required to reach equilibrium. The results presented here are useful in characterising Moringa gum filler as a possible energy source, generating chemicals, and comprehending surface fibre qualities for the purpose of creating hybrid composites.

Conclusion

The thermal stability of epoxy Moringa gum composites were studied by preparing composite materials using the hand layup technique and analyzing their thermal properties at 4, 8, 12, 16, and 20% filler content. From TGA studies, it was found that during the major stage of the decomposition process the addition of 20% Moringa gum filler to epoxy resin increased its Initial Temperature of Decomposition from 255°C to 275°C. The addition of 20% Moringa gum filler, notably raises the peak temperature to 358.8°C in the composite, as compared to that of 355.4°C in unreinforced epoxy resin. DSC studies revealed that the glass transition temperature of the epoxy + 20% Moringa gum composite increased to 75.3°C, due to the increased space occupation which weakens molecular mobility, significantly higher than the 59°C of the epoxy resin. Activation energy and frequency factor for the prepared composites were calculated using Coats Redfern, Horowitz and Broido methods and the results are quite comparable. For the increase in Moringa gum filler composition from 4 % to 20 %, the activation energy increased from 73 to 99 kJ/mol and the frequency factor increased from $2.49x10^5$ to $7.69x10^7$ due to excellent bonding between the matrix and the filler, which needs more heat to break. Kinetic parameters were also calculated and found that change in enthalpy, entropy and Gibbs free energy increased with increase in percentage weight of Moringa gum which proves the increased thermal stability of the biocomposite as compared to the epoxy resin which makes them applicable as material for designing reactors, production of gum based chemicals and understanding the properties of surface fibres for making composites.

References

1 Kaczmar J W, Pach J & Kozlowski R, Use of natural fibres as fillers for polymer composites, *Polimery*, 10 (2006) 722.

2 Baillie C, Polymer Composites and the Environment, *Green Composites*, (2004) 1.

3 Jagadeesan R, Suyambulingam I, Indran D & Siengchin S, Novel sesame oil cake biomass waste derived cellulose micro-fillers reinforced with basalt/banana fibre-based hybrid polymeric composite for lightweight applications, *Biomass Convers Biorefin*, 13 (2023) 4443.

4 Rothon R, De-Armitt C & Gilbert M, (Eds) Brydson's, *Plastics Materials Butterworth-Heinemann*, Oxford (2017).

5 Balamurugan T, Ayyadurai G K, Trilaksana H & Palani G, Enhancing mechanical performance of flax fiber/vinyl ester composites with coconut husk char: A sustainable approach for hybrid composite material, *Biomass Convers Biorefin*, (2024).

6 Sienkiewicz N, Dominic M & Parameswaranpillai J, Natural fillers as potential modifying agents for epoxy composition: A review, *Polymers*, 14 (2022) 265.

7 Rajan V V, Shanmugam M, Santhanam V & Ramkumar S, Effect of $CaCO_3$ particulate filler on the mechanical properties of surface modified coir fibre/epoxy composite, *IOP Conf Ser: Mater Sci Eng*, 988 (2020) 012046.

8 Balaji N, Gurupranes S V, Balaguru S, Jayaraman P, Natrayan L, Subbiah R & Seeniappan K, Mechanical, wear and drop load impact behaviour of Cissus quadrangularis fiber–reinforced moringa gum powder–toughened polyester composite, *Biomass Convers Biorefin*, 14(16) (2023) 1.

9 Zamani K, Kocaman S, Işık M, Soydal U, Ozmeral N & Ahmetli G, Water sorption, thermal, and fire resistance properties of natural shell-based epoxy composites, *J Appl Polym Sci*, 139 (2022) 1.

10 Qiao Y, Das O, Zhao S N, Sun T S, Xu Q & Jiang L, Pyrolysis kinetic study and reaction mechanism of epoxy glass fiber reinforced plastic by thermo gravimetric analyzer (TG) and TG–FTIR (fourier-transform infrared) techniques, *Polymers*, 12 (2020) 2739.

11 Turmanova S, Genieva S & Vlaev L, Kinetics of nonisothermal degradation of some polymer composites: Change of entropy at the formation of the activated complex from the reagents, *J Thermodyn*, 2011 (2011) 605712.

12 Nguyen T A & Nguyen T H, Banana fiber-reinforced epoxy composites: Mechanical properties and fire retardancy, *Int J Chem Eng*, 2021 (2021) 1973644.

13 Ganesh S, Gunda Y, Mohan S R J, Raghunathan V & Dhilip J D J, Influence of stacking sequence on the mechanical and water absorption characteristics of areca sheath-palm leaf sheath fibers reinforced epoxy composites, *J Nat Fibers*, 19 (2022) 1670.

14 Alothman O Y, Jawaid M, Senthilkumar K, Chandrasekar M, Alshammari B A, Fouad H, Hashem M & Siengchin S, Thermal characterization of date palm/epoxy composites with fillers from different parts of the tree, *J Mater Res Technol* , 9 (2020) 15537.

15 Al-Bayaty S A, Jubier N J & Al-Uqaily R A H, Study of thermal decomposition behavior and kinetics of epoxy/polystyrene composites by using TGA and DSC, *J Xi'an Univ Archit Technol*, 12 (2020) 1331.

16 Bera T, Acharya S K & Mishra P, Synthesis, mechanical and thermal properties of carbon black/epoxy composites, *Int J Eng Sci Technol*, 10 (2018) 12.

17 Chinnasamya V, Subramanib S P, Palaniappanc S K, Mylsamyd B & Aruchamye K, Characterization on thermal properties of glass fiber and kevlar fiber with modified epoxy hybrid composites, *J Mater Res Technol*, 9 (2020) 3158.

18 Salasinska K, Barczewski M, Gorny R & Klozinski A, Evaluation of highly filled epoxy composites modified with walnut shell waste filler, *Polym Bull*, 75 (2018) 2511.

19 Hamed A A, Saad G R, Abdelrazek F M, El-Begawy S M & Elsabee M Z, Synthesis characterization of modified epoxy resins and novel E-glass/ spectra reinforced composites, *J Sci Res Sci*, 32 (2015) 308.

20 Rangappa S M, Siengchin S, Parameswaranpillai J, Jawaid M & Ozbakkaloglu T, Lignocellulosic fiber reinforced composites: Progress, performance, properties, applications, and future perspectives, *Polym Compos*, 43 (2022) 645.

21 Du J, Gao L, Yang Y, Chen G, Guo S, Omran M, Chen J & Ruan R, Study on thermochemical characteristics properties and pyrolysis kinetics of the mixtures of waste corn stalk and pyrolusite, *Bioresour Technol*, 324 (2021) 124660.

22 Shih Y F & Chieh Y C, Thermal degradation behavior and kinetic analysis of biodegradable polymers using various comparative models, 1, *Macromol Theory Simul*, 16 (2007) 101.

23 Sultania M & Srivatava D, The effect of CTBN concentrations on the kinetic parameters of decomposition of blends of epoxy resins modified with carboxyl-terminated liquid copolymer, *J Polym Environ*, 19 (2011) 950.

24 Acikalin K, Thermogravimetric analysis of walnut shell as pyrolysis feedstock, *J Therm Anal Calorim*, 105 (2011) 145.

25 Kumar S, Gulati K, Kumar S & Singh A, Kinetic study of thermal degradation of varieties of plywood by using thermogravimetry under nitrogen atmosphere, *Int J Adv Sci Res*, 3 (2018) 177.

26 Majedi F, Wijayanti W & Hamidi N, Parameter kinetik char hasil pirolisis serbuk kayu mahoni (switenia macrophylla) dengan variasi heating rate dan 1 temperatur, *Jurnal Rekayasa Mesin*, 6 (2015) 1.

27 Raza M, Abdallah H A, Abdullah A & Abu-Jdayil B, Date palm surface fibers for green thermal insulation, *Buildings*, 12 (2022) 866.

28 Panda D S & Ansari S A, Preformulation study on the gum of moringa oleifera, *J Pharm Sci*, 11 (2013) 41.

29 Hong T, Yin J Y, Nie S P & Xie M Y, Applications of infrared spectroscopy in polysaccharide structural analysis: Progress, challenge and perspective, *Food Chem*, 12 (2021) 100168.

30 Ravikumar K & Udayakumar J, *Moringa oleifera* gum composite a novel material for heavy metals removal, *J Environ Anal Chem*, 101 (2019) 1513.

31 Nayak S & Khuntia S K, Development and study of properties of Moringa oleifera fruit fibers/ polyethylene terephthalate composites for packaging applications, *Compos Commun*, 15 (2019) 113.

32 Coats A W & Redfern J P, Kinetic Parameters from Thermogravimetric Data, *Nature*, 201 (1964) 68.

33 Ebrahimi-Kahrizsangi R & Abbasi M H, Evaluation of reliability of coats-redfern method for kinetic analysis of non-isothermal TGA, *Trans Nonferrous Met Soc China*, 18 (2008) 17.

34 Broido A, A simple, sensitive graphical method of treating thermogravimetric analysis data, *J Polym Sci Part A-2*, 7 (1969) 1761.

35 Horowitz H H & Metzger G, A new analysis of thermogravimetric traces, *Anal Chem*, 35 (1963) 1464.

36 Samy M S, Abou-El-Nadar H M, Gomaa E A & Abd-El-Hady M N, Spectral, DFT, thermal, electrochemical, and biological investigations on Cu2+, Cd2+, and Mn2+ complexes of favipiravir ligand, *Inorg Chem Commun*, 150 (2023) 110466.

37 Singh R, Confirmation of gum polysaccharide structure from *Moringa oleifera* Lam plant by periodate oxidation studies, *Int J Chem Stud*, 4 (2016) 40.

38 Fayaz H, Karthik K, Christian K G J, Kumar M A, Sivakumar A, Kaliappan S, Mohamed J S, Subbiah R & Simon Y, An investigation on the activation energy and thermal degradation of biocomposites of jute/ bagasse/coir/nano TiO2/epoxy-reinforced polyaramid fibers, *J Nanomater*, 3 (2022) 1.

39 Koley R, Kasilingam R, Sahoo S, Chattopadhyay S & Bhowmick A K, Synthesis and characterization of phenol furfural resin from *Moringa oleifera* gum and biophenol and its application in styrene butadiene rubber, *Ind Eng Chem Res*, 58 (2019) 18519.

40 Salasinska K, Barczewski M, Borucka M, Gorny R L, Kozikowshi P, Celifinski M & Gajek A, Thermal stability, fire and smoke behaviour of epoxy composites modified with plant waste fillers, *Polymers*, 11 (2019) 1234.

41 Gargol M, Klepka T, Klapiszewski L & Podkoscielna B, Synthesis and thermo-mechanical study of epoxy resin-based composites with waste fibers of hemp as an eco-friendly filler, *Polymers*, 13 (2021) 503.

42 Ibrahim M S, Sapuanand S M & Faieza A A, Mechanical and thermal properties of composites from unsaturated polyester filled with oil palm ash, *J Mech Eng Sci*, 2 (2012) 133.

43 Ben S J, Julyes J S, Sivakumar K, Mayakannan A V & Arunprakash V R, Visco-elastic, thermal, antimicrobial and dielectric behaviour of areca fibre-reinforced nano-silica and neem oil-toughened epoxy resin bio composite, *Silicon*, 13 (2021) 1703.

44 Zhang X & Huang R, Thermal decomposition kinetics of basalt fiber-reinforced wood polymer composites, *Polymers*, 12 (2020) 2283.